Hydrometallurgy 205 (2021) 105750

Contents lists available at ScienceDirect

Hydrometallurgy

journal homepage: www.elsevier.com/locate/hydromet

The BRISA process as a path for efficient copper recovery from waste PCBs

Nieves Iglesias-González *, Francisco Carranza, Alfonso Mazuelos, Rafael Romero, Juan Lorenzo-Tallafigo, Aurora Romero-García, Pablo Ramírez

Departamento de Ingeniería Química, Universidad de Sevilla, Facultad de Química, 41012 Sevilla, Spain

ARTICLE INFO

Keywords:
BRISA process
Waste PCB
Biohydrometallurgy
Copper recovery

ABSTRACT

In the present work, a two-stage biohydrometallurgical process for copper extraction from waste PCBs is developed. The main goal of this study is to check whether to separate the chemical leaching of copper with ferric iron from the regeneration of the leaching agent by bacterial oxidation of the ferrous iron is an efficient route for copper recovery from waste PCBs. To test this proposal, large waste PCBs pieces were retained in a stirred tank reactor (STR) in contact with a leaching liquor circulating at a high flow rate between this STR and a bioreactor.

The kinetics of leaching of large PCB pieces, when ferric iron is added in excess over the stoichiometric requirements, is limited by the rate of mass transfer of the leaching agent. A heterogeneous kinetic model was proposed to fit the experimental data. It was also found that by increasing the ferric iron concentration the leaching rate was increased.

Process separation has proven to be a promising configuration in which the productivity of the bioreactor has fulfilled the leaching agent demand and 90% of copper extraction was achieved in 48 h for large waste PCBs.

1. Introduction

The quality of life in today's society is strongly linked to growing technological development, the consumption of electrical and electronic equipment increases annually by 2.5 Mt (United Nations University, n. d.). The short life cycles of these devices, either due to new technological advances, the lack of reparability or the planned obsolescence of them, causes large amounts of waste. In 2014 the world generated 9.2 Mt of e-waste and, only 5 years later, in 2019, generated 53.6 Mt. Global e-waste generation is estimated to grow to 74.7 Mt by 2030.

Currently, e-waste management consists of dumping, incineration, recycling, or exporting to underdeveloped countries (Pokhrel et al., 2020; Tansel, 2017). Most of these options are unacceptable. Landfilling and incineration have a severe impact on human health and the environment through air, water, and soil pollution. Burning e-waste generates toxic gases like dioxins, furans and inorganic bromide. On the other hand, millions of poor people in underdeveloped countries are involved in manual e-waste recycling operations and most with very low levels of literacy and therefore very little awareness of the dangers of e-waste toxins (Needhidasan et al., 2014a,b). The best option for managing e-waste is correct recycling that conserves resources without affecting health or the environment.

The proper functioning and conductivity of electronic equipment are guaranteed by embedded printed circuit boards (PCB). PCBs account for 3 to 6% by weight of e-waste and are made up of approximately 40% of metals, 30% of polymers and 30% of ceramics, distributed in screen printing, solder mask, bonding materials, layers metal, and polymer substrate (Estrada-Ruiz et al., 2016; Hao et al., 2020). Metals are mostly Cu, Fe, Sn, Zn, Al, Pb, Ni, Ag, Au, and Pd; polymers are mainly phenoxy resin, polyvinyl acetate, and vinyl chloride; and ceramics mainly SiO_2, CaO, and Al_2O_3 as glass fibre (Nekouei et al., 2018).

The composition of PCBs varies considerably depending on the location, year and type of appliance in which they were used (Hubau et al., 2019). Yamane et al., 2011 analysed the chemical composition of PCBs in personal computers and mobile phones and observed copper concentrations of 20% and 34.5% by weight, respectively. The concentrations of base metals such as Cu (up to 35%) and Ni (1–3%) and precious metals such as Au (50–1500 g/t), Ag (120–5000 g/t) and Pd (about 200 g/t) in PCBs are significantly higher than those of natural deposits (Oguchi et al., 2011). Furthermore, unlike natural minerals, PCBs contain metals in their pure state, without combining and with a high copper concentration. These reasons make them very interesting potential secondary deposits.

The valuable metals contained in PCBs can be recovered by using different techniques such as pyrometallurgy, hydrometallurgy and bio-hydrometallurgy. Among all of them, bio-hydrometallurgy is

* Corresponding author.
E-mail address: mnieves@us.es (N. Iglesias-González).

https://doi.org/10.1016/j.hydromet.2021.105750
Received 11 June 2021; Received in revised form 10 September 2021; Accepted 12 September 2021
Available online 21 September 2021

considered the most environmentally friendly option (Arda et al., 2018), therefore several studies have been made in recent years to study the bioleaching of PCBs.

Nevertheless, most of the previous work in this field is devoted to studying the bioleaching of finely divided PCBs with the ferrous oxidizing bacteria in the same reactor where the PCBs are leached (Arshadi and Mousavi, 2014; Becci et al., 2021; Chen et al., 2015; Işıldar et al., 2016). In this process configuration, the microbial community has severe adaptation problems that slow down the bioleaching process (Işıldar et al., 2019). To overcome this issue, the starting hypothesis of the present work consists of the physical separation of chemical and biological actions of the bioleaching in different reactors as previously developed by the BRISA process to the copper recovery from sulphide minerals and concentrates (Carranza et al., 2004, 1997, 1993; Palencia et al., 2002; Romero et al., 2003). Among the valuables metals mentioned above, this work focuses on the recovery of Cu. In this way, the copper contained in the PCBs would be released by oxidation, in a chemical reactor, with the biogenic ferric coming from the biological reactor. Designing separately each reactor allows us to enhance their efficiencies and robustness, zero consumption of oxidizing agent (ferric iron) and water, and without generation of liquid effluents. Finally, Cu° could be obtained from the leachates by a conventional hydrometallurgical downstream processing applying solvent extraction (SX) and electrowinning (EW).

First, several batch ferric leaching tests of double-layer Fr4-PCBs and multilayer waste PCBs in an orbital shaker have been carried out to gain insight into the copper leaching kinetics from large pieces of PCBs. From these experiments, a kinetics model has been proposed and has been used to fit the experimental data obtained when the two-stage copper leaching process was performed.

A stirred tank reactor (STR) for leaching of PCBs and a flooded packed bed bioreactor (FPBB) for regeneration of leaching agent were connected in series. In the absence of cells, operating an STR at a high stirring rate and temperature is feasible without biological restrictions. Ferric iron (leaching agent) must be efficiently supplied from the bioreactor at the rates demanded by STR. The highest ferrous iron bio-oxidation rates reported in the literature were obtained in FPBB (Mazuelos et al., 1999, 2000), where cells are strongly attached to an inert solid support, thus reaching high ferrous iron conversions at high liquid flow rates. To operate at high liquid flow rates, large pieces of PCBs are used in the present study to avoid the particles being swept out of the STR by liquid flow.

2. Materials and methods

2.1. Printed circuit board samples

Two types of samples were used: double-layer FR-4 PCBs and waste multi-layer PCBs. The FR-4 PCBs, consisting of fibreglass epoxy resin covered by 18 μm copper foil on both sides (420/297/0.6 mm), were supplied by AERZETIX company. The copper content was 27 ± 1%. The FR-4 PCBs were manually cut into small pieces of 1 × 1 cm. Waste PCBs were provided by RECILEC, a local electronic waste management company in Seville, Spain. The Cu grade of the sample was between 25 and 40%. The PCBs, as received, were cut into pieces between 0.5 and 1 cm. Fig. 1 shows a simplified schematic of both PCBs used in the present study.

2.2. Culture and growth medium

The culture used in the present study consisted mainly of *A. ferrooxidans* and *Leptospirillum ferrooxidans*, and some heterotrophic bacteria, mostly related with *Acidophilium* genus (Mazuelos et al., 2012). It was originally isolated from Rio Tinto mine drainage waters (Huelva, Spain) and has been routinely maintained on a modified Silverman and Lundgren 9 K (1959) nutrient medium at pH 1.25 and 31 °C.

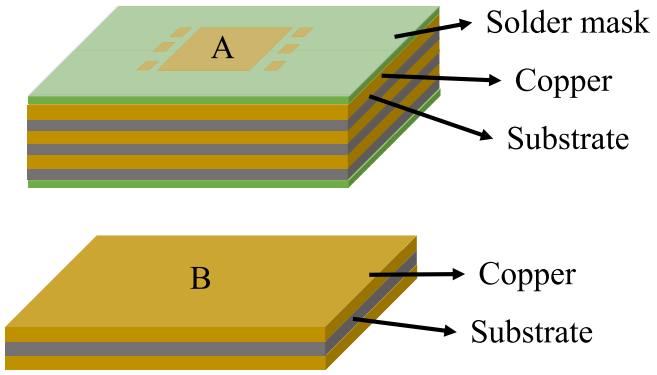

Fig. 1. Schematic of waste multi-layer PCB (A) and double-layer FR-4 PCB (B).

2.3. Flooded packed-bed bioreactor

Flooded packed-bed bioreactors have been developed for the oxidation of ferrous ion, achieving steady states and very high oxidation rates without any supply of cells (Mazuelos et al., 1999, Mazuelos et al., 2000). The flooded packed-bed bioreactor (FPBB) enables immobilization of biomass in a biofilm that covers the surfaces of the particles of the bed (Mazuelos et al., 2012). This biofilm consists of an inorganic matrix of precipitated ferric compounds, mainly oxyhydroxides and jarosites, where cells are attached (Daoud and Karamanev, 2006).

The FPBB (Fig. 2) is a column made up of polymethyl methacrylate tube of 14 cm in height and 8.4 cm in diameter, with a lower chamber (hollow cylindrical, 5.8 cm in height), at the bottom and an upper chamber packed with inert siliceous stone particles (particle size 6–8 mm) as biomass support. The bed porosity is 0.42. The lower chamber has two nozzles for feeding air and liquid. This stream goes up through the bed flooding it. The liquid is fed by a peristaltic pump and air by a small compressor controlled by a rotameter (750 mL/min). Solution outlet was placed at the top of the column (by overflow). The reactor is placed in a thermostatic chamber at 31 °C. To fix the cells to the siliceous particles, the procedure proposed by Mazuelos et al. (2001) was carried out.

2.4. Ferric leaching tests of FR-4 PCBs

For the leaching tests, 250 ml Erlenmeyer flasks in an orbital incubator with temperature control were used at a shaking speed of 180 rpm. To study the influence of temperature, a plate of FR-4 PCB has been used

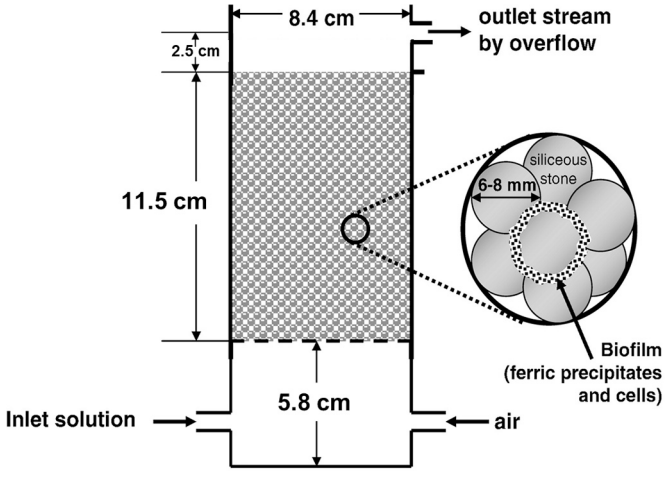

Fig. 2. Schematic of flooded packed bed bioreactor (Adapted from Iglesias et al., 2016 with permission of Elsevier).

in each experiment in a volume of 100 mL of bio-oxidised 9 K medium as a leaching solution. The tested temperatures have been 30, 40, 50 and 60 °C. In each test, the concentration of dissolved copper as a function of time was measured to obtain the kinetic curves.

2.5. Leaching of waste PCBs with continuous biological regeneration of ferrous ion

A schematic representation of the experimental device used is shown in Fig. 3. This experimental setup was placed in a thermostated chamber at 31 °C.

The experimental device (Fig. 3) consists of a 1 L-STR and the FPBB connected in series, with continuing recycling of the liquid between both reactors. The STR outlet stream was pumped by a peristaltic pump at the bottom of FPBB. The FPBB outlet stream was returned by overflow to the STR.

The STR was initially fed with biogenic ferric iron solution at pH 1.25 and waste PCBs with a solid/liquid ratio of 2.5% (*w/v*). Two tests were carried out at different ferric iron concentrations: 9 and 20 g/L.

Copper concentrations and ORP were measured inside the chemical reactor and at the top of the bioreactor.

2.6. Analysis and control

The PCB samples and leach residues were subjected to acid digestion with aqua regia to determine the copper grade. Copper was measured by atomic absorption spectrophotometry (2380 spectrophotometer, Perkin Elmer). Ferric iron concentration was determined by the sulfosalicylic acid method and ferrous iron concentration was determined by automatic titration with $K_2Cr_2O_7$.

3. Results

3.1. Batch leaching of FR-4 PCBs

Fig. 4 shows the kinetics of the oxidation of copper from FR-4 PCB pieces in Erlenmeyer flasks with 0.1 L of 9 g/L biogenic ferric sulphate at pH = 1.25 at the four temperatures studied: 30 °C (Fig. 3A), 40 °C (Fig. 3B), 50 °C (Fig. 3C) and 60 °C (Fig. 3D). The copper content of the PCB pieces is in the range 38 and 42 mg for all the experiments, thus the ferric iron is in a high excess over its stoichiometric value required to leach copper in all the tests. In this way, the oxidation-reduction potential (ORP) values were over 700 mV (vs. NHE). Before carrying out these experiments it was checked that the PCB pieces were not leached with sulphuric acid alone at pH 1.25 (data not shown).

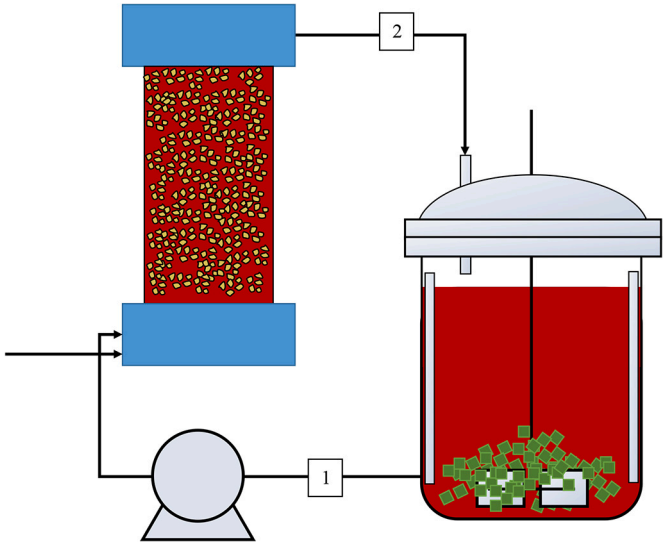

Fig. 3. Schematic of the two-stage system used in the present study. Samples were taken from streams 1 (outlet of the STR) and stream 2 (outlet of the FPBB).

It is seen (Fig. 4) that all the copper is leached at the four temperatures studied in less than one hour. Two different regimes are observed: first, the copper conversion, X_{Cu}, increases linearly with time, whereby copper is oxidized at a constant rate; second, the rate of oxidation gradually decreases to zero. The onset of the second regime is related to the beginning of the removal of the copper layer, which advances from the edges of the sheet to the centre of it as it has been experimentally observed (see Fig. S1 of the supplementary material). Therefore, the experimental data were fitted to a heterogeneous kinetic model that takes into account the two observed regimes, a first one where the surface area is constant and equal to $A_{\max}$ and a second one where the surface area is proportionally reduced with the dissolution of copper. The start of the second regime is assumed to take place for a given copper conversion value, $X_{Cu,ref}$

$$\begin{aligned} \frac{dX_{Cu}}{dt} &= \frac{1}{2}\cdot k_{ef}\cdot\frac{A_{\max}}{V}\cdot\frac{\left[Fe^{3+}\right]}{\left[Cu^{2+}\right]_{\max}} \quad \text{if } X_{Cu} < X_{Cu,ref} \\ \frac{dX_{Cu}}{dt} &= \frac{1}{2}\cdot k_{ef}\cdot\frac{A_{\max}}{V}\cdot\frac{(1-X_{Cu})}{(1-X_{Cu,ref})}\cdot\frac{\left[Fe^{3+}\right]}{\left[Cu^{2+}\right]_{\max}} \quad \text{if } X_{Cu} \geq X_{Cu,ref} \end{aligned} \tag{1}$$

where k_{ef} is the effective transport coefficient (cm/min), X_{Cu} is the fraction of copper leached from the PCB sheet, A_{max} stands for the maximum area of the copper sheet exposed to the ferric sulphate solution (cm^2), V is the volume of the ferric solution (cm^3), $[Fe^{3+}]$ is the bulk concentration of ferric iron (g/L), $[Cu^{2+}]_{\max}$ is the final concentration of cupric ions in the solution once all the copper has been leached (g/L), 1/2 is the stoichiometric relation between Cu^{2+} and Fe^{3+} ($Cu_{(s)}{}^0 + 2Fe_{(aq)}{}^{3+} \rightarrow Cu_{(aq)}{}^{2+} + 2Fe_{(aq)}{}^{2+}$) and $X_{Cu,ref}$ is the copper conversion at which the second regime begins. Furthermore, the ratio $\frac{[Fe^{3+}]}{[Cu^{2+}]_{\max}}$ can be expressed as a function of copper conversion:

$$\frac{\left[Fe^{3+}\right]}{\left[Cu^{2+}\right]_{\max}} = \frac{\left[Fe^{3+}\right]_0}{\left[Cu^{2+}\right]_{\max}} - 2\cdot\frac{AW(Fe)}{AW(Cu)}X_{Cu} \tag{2}$$

where $[Fe^{3+}]_0$ is the initial ferric ion concentration (g/L) and AW(Fe) and AW(Cu) are the atomic weight of iron and copper, respectively.

The lines in Fig. 3 shows the best fit to the experimental data obtained by non-linear regression of Eqs (1) and (2), with the rate constant $k' = \frac{1}{2}\cdot k_{ef}\cdot\frac{A_{\max}}{V}(\min^{-1})$ and $X_{Cu,ref}$ as the adjusting parameters. Table 1 shows the parameters obtained along with their 95% confidence interval.

To determine whether the reaction rate is mass transfer limited, the dependence of k' with temperature was studied. Fig. 5 shows the Arrhenius plot where $\ln k'$ vs. $1/T$, being T the absolute temperature, has been displayed. From the slope of this plot an activation energy (E_a) of 16.9 kJ/mol was obtained. This low E_a indicates that the reaction is limited by mass transfer. Furthermore, this value is in good agreement with the activation energy obtained in a previous study of the leaching kinetics of copper from waste PCBs (Yazici and Deveci, 2014).

3.2. Batch leaching of multilayer waste PCBs

Fig. 6 shows the kinetics of copper leaching from multilayer waste PCBs in the Erlenmeyer flasks with 0.1 L of 9 g/L biogenic ferric sulphate at pH = 1.25 at 30 °C for two independent experiments. The copper weight of the PCBs was 85 mg (circles) and 100 mg (squares), so the ferric iron was at high excess from stoichiometric value and ORP values remained over 700 mV (vs. NHE).

In both tests, the kinetics of copper leaching is likely to be slowed down by the occurrence of internal mass transfer limitations.

Therefore, the kinetics of copper leaching can be modelled as a combination of an external and internal mass transfer process that takes

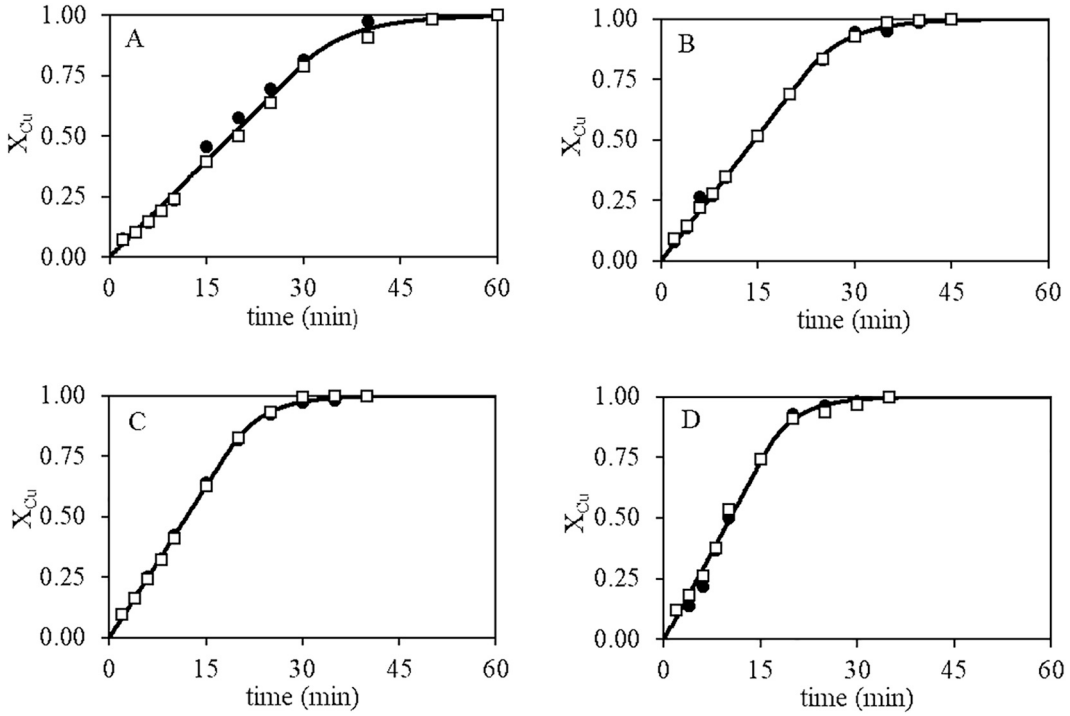

Fig. 4. Copper dissolution kinetics of two-layer FR-4 PCBs at four temperatures: 30 °C (Fig. 4A), 40 °C (Fig. 4B), 50 °C (Fig. 4C) and 60 °C (Fig. 4D). The kinetics were studied in 0.25 L Erlenmeyer flasks placed in an orbital shaker with temperature control at a shaking rate of 180 rpm. As an oxidizing solution, 0.1 L of 9 g/L biogenic ferric sulphate at pH 1.25 was used. Two experiments were carried out at each temperature (symbols). The lines are those that best fit the experimental data according to the heterogeneous kinetic model explained in the text.

Table 1
Values of the adjusting parameters used to fit the experimental data in Fig. 4 to the heterogeneous kinetic model given by Eqn (1) and (2).

T(°C)	$k' \cdot 10^3$ (h^{-1})	$X_{Cu,ref}$
30	72.0 ± 0.02	0.80 ± 0.09
40	93.6 ± 0.02	0.80 ± 0.04
50	112.8 ± 0.01	0.80 ± 0.02
60	132 ± 6	0.8 ± 0.1

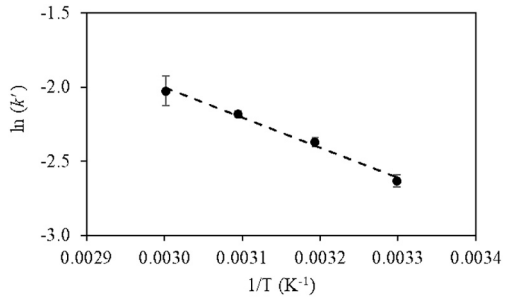

Fig. 5. Arrhenius plot of the kinetics constants, k'. The dashed line is the linear regression of the experimental data from where an activation energy, E_a, of 16.9 kJ/mol has been obtained.

place simultaneously:

$$\frac{dX_{Cu}}{dt} = \left(k'_{ex} + k'_{in}\right)\frac{[Fe^{3+}]}{[Cu^{2+}]_{max}} \quad (3)$$

where k'_{ex} and k'_{in} are the mass transfer coefficients for the external and internal mass transfer process, respectively (h^{-1}), and [Fe^{3+}] is the ferric iron concentration in the Erlenmeyer flask (g/L).

On the one hand and according to the heterogeneous kinetic model

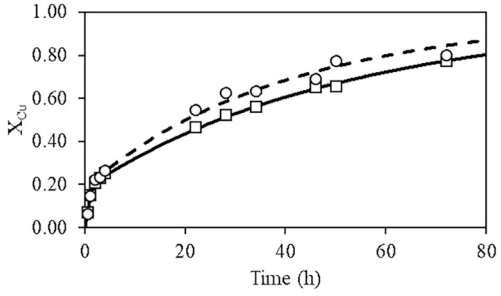

Fig. 6. Copper dissolution kinetics of multilayer waste PCBs at 30 °C for two independent experiments. The kinetics were studied in 0.25 L Erlenmeyer flasks placed in an orbital shaker with temperature control at a shaking rate of 180 rpm. As an oxidizing solution, 0.1 L of 9 g/L biogenic ferric sulphate at pH 1.25 was used. The lines are those that best fit the experimental data according to the model explained in the text with the adjusting parameters given in Table 2.

used for the FR-4 PCBs, the external mass transfer coefficient will be constant until a critical copper conversion value is reached ($X_{Cu,ref} = 0.8$) from that copper conversion value the mass transfer coefficient decreases linearly with the copper conversion. On the other hand, the internal mass transfer coefficient will be considered to decrease linearly with the inner copper leached. Therefore, the external and internal mass transfer coefficients can be approximated by the following expressions:

$$k'_{ex} = k'_{ex,max} \quad \text{if } X_{Cu,ex} < 0.8$$
$$k'_{ex} = k'_{ex,max}\cdot\frac{(1 - X_{Cu,ex})}{(1 - 0.8)} \quad \text{if } X_{Cu,ex} \geq 0.8 \quad (4)$$

$$k'_{in} = k'_{in,max}\cdot\left(1 - X_{Cu,in}\right) \quad (5)$$

where $k'_{ex,max}$ and $k'_{in,max}$ are the maximum values of the mass transfer coefficients for the external and internal mass transfer process (h^{-1});

$X_{Cu,ex}$ and $X_{Cu,in}$ are the copper conversion of the external and internal copper, and can be determined as follows:

$$X_{Cu,ex} = \frac{m_{Cu,ex}}{\alpha \cdot m_{Cu,max}}$$
$$X_{Cu,in} = \frac{m_{Cu,in}}{(1-\alpha)\cdot m_{Cu,max}} \quad (6)$$

where $m_{Cu,ex}$ and $m_{Cu,\ in}$ are the mass of the external and internal copper (g), respectively. $m_{Cu,max}$ stands for the total mass of copper in the waste PCBs (g) and α is the fraction of the total mass of copper that belongs to the external copper.

Finally, the ratio $\frac{[Fe^{3+}]}{[Cu^{2+}]_{max}}$ is obtained from Eq. (2).

It is seen (Fig. 5) that the proposed model fit well with experimental data with the adjusting parameters given in Table 2.

3.3. Batch leaching of multilayer waste PCBs aided by a ferrous oxidation bioreactor

The main goal of the present study was to check whether the copper from waste PCBs could be efficiently leached in a close circuit where the bio-oxidation of the ferrous iron is carried out in a separate FPBB, avoiding the direct contact of the bacteria with the PCBs that could cause inhibition for the bacterial growth and, therefore, a decrease of the bio-oxidation rate. Moreover, to be able to feed the chemical reactor at a high flow rate, the idea was to work with large PCBs pieces which can be easily kept in the chemical reactor without entering the FPBB (see the scheme of the process in Fig. 3).

Furthermore, from the preliminary experiments using Erlenmeyer flask it was shown that, if the ferric iron concentration is kept at a high value, the oxidation kinetics is diffusion-controlled and, therefore, should be a function of the bulk ferric iron concentration, as well as other factors. Bearing this in mind two different tests have been carried out with two initial ferric iron concentrations: 9 g/L and 20 g/L. Fig. 6 shows the evolution of the ferric iron concentration over time for both tests. The ferric iron concentration was measured at points 1 (circles) and 2 (squares) of the process scheme (Fig. 3). Ferric iron concentration at point 1 was equal to the ferric iron concentration in the STR ($[Fe^{3+}]_{STR}$) whereas the ferric iron concentration at point 2 was equal to the ferric iron concentration in the FPBB ($[Fe^{3+}]_{FPBB}$) since the flow behaviour of this reactor is close to a perfect mixed reactor as shown in a previous study (Mazuelos et al., 2019). It is seen that this configuration process allows us to have a high ferric iron concentration for all the experimental time in the STR since the FPBB was able to regenerate it at the rate demanded, keeping a practically constant ferric iron concentration in the feed to the STR (squares in Fig. 7).

Fig. 8 shows the copper leaching kinetics for the two tests of multilayer waste PCBs in the STR + FPBB system. The kinetics resembles the one obtained from the Erlenmeyer flask shown in Fig. 6. Therefore, the experimental data were modelled by using Eqs (3) to (6). The ferric iron concentration in Eq. (3) corresponds in this system to the ferric iron concentration in the STR. The ferric iron concentration in the STR is given by a mass balance of the ferric iron:

$$\frac{d[Fe^{3+}]_{STR}}{dt} = \frac{\nu}{V_{STR}}\cdot\left([Fe^{3+}]_{FPBB} - [Fe^{3+}]_{STR}\right) - 2\frac{AW(Fe)}{AW(Cu)}\cdot[Cu^{2+}]_{max}\cdot\frac{dX_{Cu}}{dt} \quad (7)$$

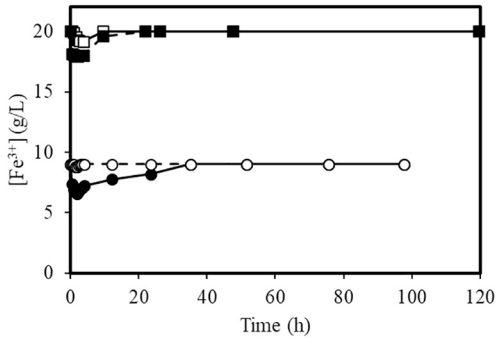

Fig. 7. Ferric iron concentration as a function of reaction time for the copper leaching of multilayer waste PCBs in the STR aided by the FPBB as shown in Fig. 3. Squares are the data for the reaction carried out at 9 g/L initial ferric iron concentration, whereas circles show the results for the experiment with 20 g/L of initial ferric iron. In both figures, closed symbols are the ferric iron concentration values in the STR, whereas the open symbols stand for the ferric iron concentration values in the FPBB.

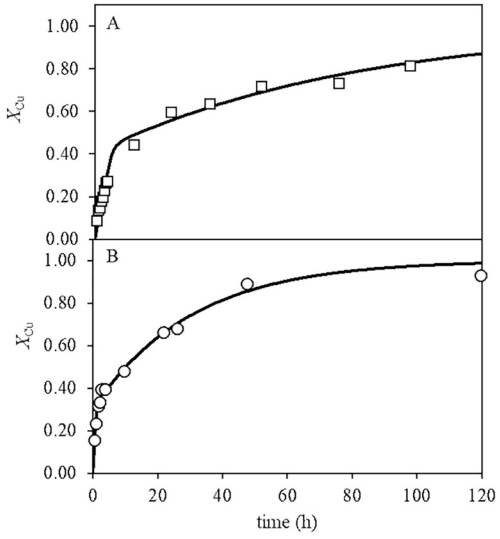

Fig. 8. Copper leaching kinetics for multilayer PCB waste in a stirred tank reactor aided with a ferrous oxidation bioreactor. Experimental conditions: T = 30 °C, stirring rate = 500 rpm; solid/liquid ratio in the STR = 2.5%; ferric concentration: (A) 9 g/ L and (B) 20 g/ L. Lines show the best fit of the experimental data to the model in Eqs 3 - 7 with the parameters given in Table 3.

where ν is the volumetric flow rate (L/h), V_{STR} is the volume of the STR (L), AW(Fe) and AW(Cu) are the atomic weight of iron and copper, respectively, 2 is the stoichiometric coefficient of the iron and $[Fe^{3+}]_{FPBB}$ is the ferric iron concentration in the outlet stream of the FPBB. Fig. 7 shows that $[Fe^{3+}]_{FPBB}$ remained practically constant and equal to the initial ferric iron concentration for both experiments, therefore $[Fe^{3+}]_{FPBB}$ can be assumed to be constant and equal to $[Fe^{3+}]_0$.

Eqs (4) to (7) were solved simultaneously with the initial conditions: $X_{Cu} = 0$ and $[Fe^{3+}]_{STR} = [Fe^{3+}]_0$. The lines in Fig. 8A and B show the best fit to the experimental data with the values of the adjusting parameters

Table 2
Values of the adjusting parameters used to fit the experimental data in Fig. 4 to the heterogeneous kinetic model given by Eqs (2) to (6).

Experiment	$k'_{ex,max}\cdot10^3$ (h^{-1})	$k'_{in,max}\cdot10^3$ (h^{-1})	α
1	14 ± 5	2.4 ± 0.3	0.18 ± 0.04
2	12 ± 2	1.5 ± 0.1	0.18 ± 0.01

Table 3
Values of the adjusting parameters used to fit the experimental data in Fig. 8 to the heterogeneous kinetic model given by s. Eqs (3) to (7).

$[Fe^{3+}]_0$ (g/L)	k'_{ex} (h^{-1})	$k'_{in}\cdot10^3$ (h^{-1})	α
9	0.11 ± 0.02	9 ± 4	0.42 ± 0.08
20	0.08 ± 0.02	8 ± 2	0.31 ± 0.04

given in Table 3.

It is seen that the proposed model fit the experimental data. Furthermore, the internal and external mass transfer coefficients have the same values within the experimental error for both experiments confirming the reliability of the model. The only parameter that differs from both experiments is the fraction of external copper, which indicates that there is a higher fraction in the experiment conducted with 9 g/L ferric iron concentration, which showed a higher surface area of the exposed copper from the waste PCB sample, compared to that in the experiment with 20 g/L ferric ion concentration.

It is worth noting that increasing ferric iron concentration improves copper leaching kinetics. For the experiment at a ferric iron concentration of 20 g/L, a copper extraction of 90% was achieved at 48 h with an average copper oxidation rate of 126 mg/L h^{-1}, whereas for the 9 g/L test only an 80% copper conversion was reached in 96 h.

Fig. 9 shows ferrous conversion ($X_{Fe}{}^{2+}$) at the FPBB (left axis) and the overall copper concentration (right axis) for the two experiments with different concentrations of iron (Fig. 9A – 9 g/L and Fig. 9B – 20 g/L). It is seen that for the experiment at 9 g/L the ferrous conversion is practically complete for all the experimental interval, whereas, for the experiment at 20 g/L the ferrous conversion decreases at the beginning of the experiment reaching a minimum conversion value of 0.6. It is clear that increasing ferric iron concentration from 9 g/L to 20 g/L increases the copper leaching rate so the ferric consumption rate in the STR is higher than the ferrous oxidation rate in the FPBB leading to a decrease in the ferrous conversion for the experiment at 20 g/L.

To explore the ferric iron generation rate in the FPBB the following equation was used:

$$\text{generation rate (g/h)} = \nu \cdot \left([Fe^{2+}]_{in} - [Fe^{2+}]_{out} \right) \quad (8)$$

where ν is the liquid flow rate, $[Fe^{2+}]_{in}$ and $[Fe^{2+}]_{out}$ are the ferrous iron concentrations at the inlet and outlet streams of the FPBB, respectively. It is shown in Fig. 10 that the generation rate for both experiments reach a maximum value at the beginning followed by a marked decrease in the productivity that becomes practically zero at larger times when the copper leaching kinetics in the STR was governed by the internal mass transfer. The inset of Fig. 10 shows the generation rate values for the first 5 h when the copper leaching kinetics is mainly due to the external mass transfer of ferric iron. It is seen that the generation rate is slightly higher (0.85 g/h) for the experiment at 20 g/L of ferric iron than for the experiment at 9 g/L (0.77 g/h). Therefore, the FPBB has shown that can produce ferric iron at a rate between 0.85 and 0.77 g Fe^{3+}/h which correspond to the rate of consumption of ferric iron needed to leach the copper from PCBs at rates ranging between 0.42 and 0.46 g Cu^{2+}/h, which would be the copper leaching rate that can be kept by the regeneration of Fe^{3+} in the FPBB if copper leaching kinetics in the STR were not slowed down by internal mass transfer.

4. Conclusions

The present study aimed to check whether the physical separation of chemical and biological actions of the bioleaching in different reactors could be a promising option for efficient copper extraction from PCBs. Furthermore, instead of using finely divided PCBs that can cause bacterial growth inhibition, large PCB pieces were used.

It was seen that for both types of PCBs the kinetics is limited by the rate of mass transfer of ferric iron from bulk fluid to the copper surface. A kinetic model has been proposed and has been successfully used to fit the experimental data for the two-stage copper leaching from waste PCBs. Furthermore, it was proved that with increasing ferric iron concentration the rate of copper leaching increases.

Using the BRISA process, the biological reactor was able to supply the ferric iron at the rate demanded in the STR. The rate-limiting process was seen to be the chemical leaching of copper in the STR, due to the process of ferric iron mass transfer from the bulk solution to the copper surface inside the large pieces of PCB.

These findings indicate that by using a two-stage configuration copper extraction is not limited by the biological process with the experimental conditions used in this work. Therefore, further studies should be carried out to improve the chemical reactor performance, which could be achieved by reducing the size of the PCB pieces or increasing the reaction temperature always taking into account the economic aspects.

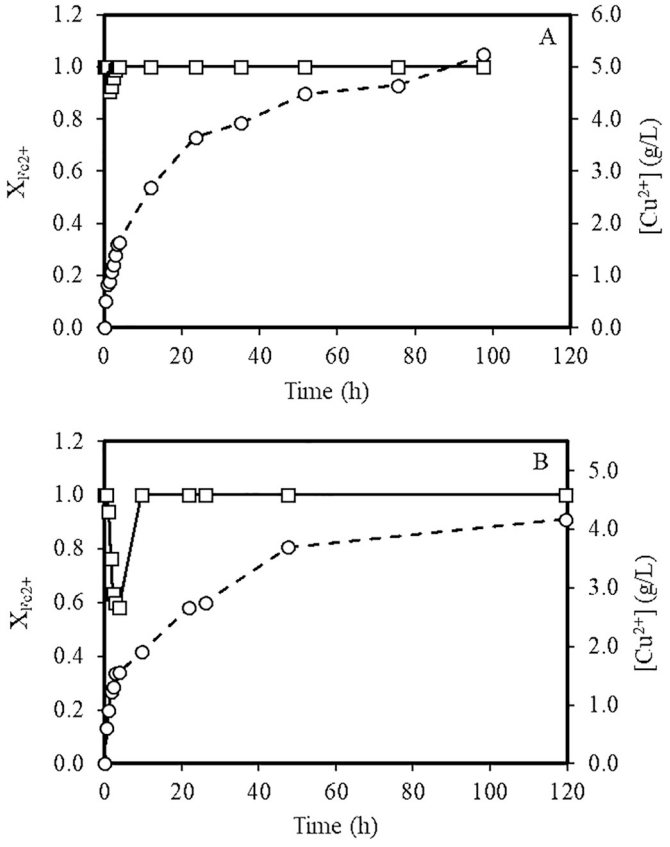

Fig. 9. Ferrous conversion at the FPBB (squares + solid lines) and overall copper concentration (circles + dashed lines). Experimental conditions: T = 30 °C, stirring rate = 500 rpm; solid/liquid ratio in the stirred tank reactor = 2.5%; ferric concentration: (A) 9 g/ L and (B) 20 g/ L.

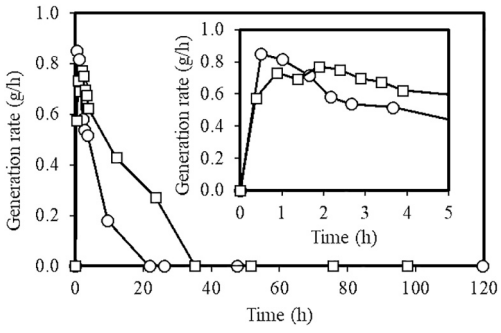

Fig. 10. Ferric iron generation rate at the FPBB. Circles are the data for the reaction carried out at 9 g/L initial ferric iron concentration, whereas squares show the results for the experiment with 20 g/L of initial ferric iron. For the shake of clarity, the inset shows the ferric iron generation rate for the first 5 h.

Author's statements

All authors have seen and approved the final version of the manuscript being submitted. They warrant that the article is the authors' original work, hasn't received prior publication and isn't under consideration for publication elsewhere.

Declaration of Competing Interest

The authors declare that they have no known competing financial interests or personal relationships that could have appeared to influence the work reported in this paper.

Appendix A. Supplementary data

Supplementary data to this article can be found online at https://doi.org/10.1016/j.hydromet.2021.105750.

References

Arda, I., Rene, E.R., Van Hullebusch, E.D., Lens, P.N.L., 2018. Resources, conservation & recycling electronic waste as a secondary source of critical metals. Manag. Recov. Technol. 135, 296–312. https://doi.org/10.1016/j.resconrec.2017.07.031.

Arshadi, M., Mousavi, S.M., 2014. Bioresource technology simultaneous recovery of Ni and Cu from computer-printed circuit boards using bioleaching. Statist. Evaluat. Optimiz. 174, 233–242. https://doi.org/10.1016/j.biortech.2014.09.140.

Becci, A., Amato, A., Rodr, M., Beolchini, F., 2021. Bioleaching of End-of-Life Printed Circuit Boards: Mathematical Modeling and Kinetic Analysis. https://doi.org/10.1021/acs.iecr.0c05566.

Carranza, F., Iglesias, N., Romero, R., Palencia, I., 1993. Kinetics improvement of high-grade sulphides bioleaching by effects separation. FEMS Microbiol. Rev. 11, 129–138. https://doi.org/10.1111/j.1574-6976.1993.tb00276.x.

Carranza, F., Palencia, I., Romero, R., 1997. Silver catalyzed IBES process: application to a Spanish copper–zinc sulphide concentrate. Hydrometallurgy 44, 29–42. https://doi.org/10.1016/S0304-386X(96)00028-X.

Carranza, F., Iglesias, N., Mazuelos, A., Palencia, I., Romero, R., 2004. Treatment of copper concentrates containing chalcopyrite and non-ferrous sulphides by the BRISA process. Hydrometallurgy 71, 413–420. https://doi.org/10.1016/S0304-386X(03)00119-1.

Chen, S., Yang, Y., Liu, C., Dong, F., Liu, B., 2015. Chemosphere column bioleaching copper and its kinetics of waste printed circuit boards (WPCBs) by Acidithiobacillus ferrooxidans. Chemosphere 141, 162–168. https://doi.org/10.1016/j.chemosphere.2015.06.082.

Daoud, J., Karamanev, D., 2006. Formation of jarosite during Fe2+ oxidation by Acidithiobacillus ferrooxidans. Miner. Eng. 19, 960–967. https://doi.org/10.1016/j.mineng.2005.10.024.

Estrada-Ruiz, R.H., Flores-Campos, R., Gámez-Altamirano, H.A., Velarde-Sánchez, E.J., 2016. Separation of the metallic and non-metallic fraction from printed circuit boards employing green technology. J. Hazard. Mater. 311, 91–99. https://doi.org/10.1016/j.jhazmat.2016.02.061.

Hao, J., Wang, Y., Wu, Y., Guo, F., 2020. Resources, conservation & recycling metal recovery from waste printed circuit boards: A review for current status and perspectives. Resour. Conserv. Recycl. 157, 104787. https://doi.org/10.1016/j.resconrec.2020.104787.

Hubau, A., Chagnes, A., Minier, M., Touzé, S., Chapron, S., Guezennec, A., 2019. Recycling-oriented methodology to sample and characterize the metal composition of waste printed circuit boards. Waste Manag. 91, 62–71. https://doi.org/10.1016/j.wasman.2019.04.041.

Iglesias, N., Romero, R., Montes-Rosua, C., Carranza, F., 2016. Treatment of tetrathionate effluents by continuous oxidation in a flooded packed-bed bioreactor. Int. J. Miner. Process. 155, 91–98.

Işıldar, A., van de Vossenberg, J., Rene, E.R., van Hullebusch, E.D., Lens, P.N.L., 2016. Two-step bioleaching of copper and gold from discarded printed circuit boards (PCB). Waste Manag. 57, 149–157. https://doi.org/10.1016/j.wasman.2015.11.033.

Işıldar, A., van Hullebusch, E.D., Lenz, M., Du Laing, G., Marra, A., Cesaro, A., Panda, S., Akcil, A., Kucuker, M.A., Kuchta, K., 2019. Biotechnological strategies for the recovery of valuable and critical raw materials from waste electrical and electronic equipment (WEEE) – a review. J. Hazard. Mater. 362, 467–481. https://doi.org/10.1016/j.jhazmat.2018.08.050.

Mazuelos, A., Palencia, I., Romero, R., Rodriguez, G., Carranza, F., 2001. Ferric iron production in packed bed bioreactors: influence of pH, temperature, particle size, bacterial support material, and type of air distributor. Miner.Eng. 14 (5), 507–514.

Mazuelos, A., Romero, R., Palencia, I., Iglesias, N., Carranza, F., 1999. Continuous ferrous iron biooxidation in flooded packed bed reactors. Miner. Eng. 12, 559–564. https://doi.org/10.1016/S0892-6875(99)00037-0.

Mazuelos, A., Moreno, J.M., Carranza, F., Palomino, C., Torres, A., Villalobo, E., 2012. Biotic factor does not limit operational pH in packed-bed bioreactor for ferrous iron biooxidation. J. Ind. Microbiol. Biotechnol. 39, 1851–1858. https://doi.org/10.1007/s10295-012-1187-9.

Mazuelos, A., Carranza, F., Palencia, I., Romero, R., 2000. High efficiency reactor for the biooxidation of ferrous iron. Hydrometallurgy 58, 269–275.

Mazuelos, A., García-Tinajero, C.J., Romero, R., Iglesias-González, N., Carranza, F., 2019. Causes of inhibition of bioleaching by cu are also thermodynamic. J. Chem. Technol. Biotechnol. 94, 185–194. https://doi.org/10.1002/jctb.5761.

Needhidasan, S., Samuel, M., Chidambaram, R., 2014a. Electronic Waste-an Emerging Threat to the Environment of Urban India. https://doi.org/10.1186/2052-336X-12-36.

Needhidasan, S., Samuel, M., Chidambaram, R., 2014b. Electronic Waste-an Emerging Threat to the Environment of Urban India. https://doi.org/10.1186/2052-336X-12-36.

Nekouei, R.K., Pahlevani, F., Rajarao, R., Golmohammadzadeh, R., Sahajwalla, V., 2018. Two-step pre-processing enrichment of waste printed circuit boards: mechanical milling and physical separation. J. Clean. Prod. 184, 1113–1124. https://doi.org/10.1016/j.jclepro.2018.02.250.

Oguchi, M., Murakami, S., Sakanakura, H., Kida, A., Kameya, T., 2011. A preliminary categorization of end-of-life electrical and electronic equipment as secondary metal resources. Waste Manag. 31, 2150–2160. https://doi.org/10.1016/j.wasman.2011.05.009.

Palencia, I., Romero, R., Mazuelos, A., Carranza, F., 2002. Treatment of secondary copper sulphides (chalcocite and covellite) by the BRISA process. Hydrometallurgy 66, 85–93. https://doi.org/10.1016/S0304-386X(02)00095-6.

Pokhrel, P., Lin, S.L., Tsai, C.T., 2020. Environmental and economic performance analysis of recycling waste printed circuit boards using life cycle assessment. J. Environ. Manag. 276, 111276. https://doi.org/10.1016/j.jenvman.2020.111276.

Romero, R., Mazuelos, A., Palencia, I., Carranza, F., 2003. Copper recovery from chalcopyrite concentrates by the BRISA process. Hydrometallurgy 70, 205–215. https://doi.org/10.1016/S0304-386X(03)00081-1.

Tansel, B., 2017. From electronic consumer products to e-wastes: global outlook, waste quantities, recycling challenges. Environ. Int. https://doi.org/10.1016/j.envint.2016.10.002.

United Nations University, n.d. Ewastemonitor [WWW Document]. URL http://ewastemonitor.info/wp-content/uploads/2020/06/GEM_2020_Executive_summery.pdf (accessed 5.20.21).

Yamane, L.H., Moraes, V.T.D., Crocce, D., Espinosa, R., Alberto, J., Tenório, S., 2011. Recycling of WEEE : characterization of spent printed circuit boards from mobile phones and computers. Waste Manag. 31, 2553–2558. https://doi.org/10.1016/j.wasman.2011.07.006.

Yazici, E.Y., Deveci, H., 2014. Ferric sulphate leaching of metals from waste printed circuit boards. Int. J. Miner. Process. 133, 39–45. https://doi.org/10.1016/J.MINPRO.2014.09.015.